

# Amplitude variability in satellite photometry of the non-radially pulsating O9.5 V star $\zeta$ Oph

Ian D. Howarth,<sup>1</sup>\* K. J. F. Goss<sup>2</sup>, I. R. Stevens<sup>2</sup>, W. J. Chaplin<sup>2</sup>, and Y. Elsworth<sup>2</sup>

<sup>1</sup>*Dept. Physics & Astronomy, University College London, Gower St., London WC1E 6BT*

<sup>2</sup>*School of Physics and Astronomy, University of Birmingham, Edgbaston, Birmingham B15 2TT*

27 February 2014

## ABSTRACT

We report a time-series analysis of satellite photometry of the non-radially pulsating Oe star  $\zeta$  Oph, principally using data from *SMEI* obtained 2003–2008, but augmented with *MOST* and *WIRE* results. Amplitudes of the strongest photometric signals, at 5.18, 2.96, and 2.67 d<sup>−1</sup>, each vary independently over the 5<sup>1/2</sup>-year monitoring period (from  $\sim 30$  to  $\lesssim 2$  mmag at 5.18 d<sup>−1</sup>), on timescales of hundreds of days. Signals at 7.19 d<sup>−1</sup> and 5.18 d<sup>−1</sup> have persisted (or recurred) over at least two and three decades, respectively. Supplementary spectroscopic observations show an H $\alpha$  emission episode in 2006; this coincided with small increases in amplitudes of the three strongest photometric signals.

**Key words:** Asteroseismology, techniques: photometric, stars: oscillations, stars: emission line, Be, stars: activity, stars: individual:  $\zeta$  Oph

## 1 INTRODUCTION

$\zeta$  Oph<sup>1</sup> is the nearest O-type star, and one of the brightest ( $\pi = 8.91 \pm 0.20$  mas, van Leeuwen 2007; O9.5 Vnn,  $V \simeq 2.6$ , Sota et al. 2011). Detailed spectroscopic investigations of velocity-resolved absorption-line structure have been facilitated by its brightness and exceptionally rapid rotation ( $v_e \sin i \gtrsim 400$  km s<sup>−1</sup>; Howarth & Smith 2001, Villamariz & Herrero 2005); periodic line-profile variability, discovered by Walker et al. (1979), has subsequently been widely interpreted in terms of non-radial pulsations (NRP; Vogt & Penrod 1983, Reid et al. 1993, Kambe et al. 1997). H $\alpha$  emission episodes lasting, typically, several weeks have been observed to occur every few years (e.g., Ebbets 1981; Kambe et al. 1993); the inferred circumstellar decretion disk is probably causally associated with rapid rotation, and possibly with NRP (Cranmer 2009), though the latter remains an open issue.

Spectroscopic line-profile variability associated with NRP is primarily sensitive to sectoral pulsation modes (since tessellar modes readily lead to cancellation in velocity space). Moreover, the requirements of high signal-to-noise ratio and high resolution typically limit spectroscopic time series to only a few nights, resulting in further detection biases, towards short periods and large amplitudes. These observational constraints contrast with satellite-based photometry, which can yield precise measurements over an extended time

period, thereby affording the opportunity to investigate pulsation characteristics in a parameter space inaccessible to spectroscopic study. For  $\zeta$  Oph, this opportunity was exploited by Walker et al. (2005), who found a number of periodic signals in 24 days of high-cadence, near-continuous photometry from the *Microvariability and Oscillations of STars* (*MOST*) satellite. Here we report new results from the *Solar Mass Ejection Imager* (*SMEI*) and *Wide-field InfraRed Explorer* (*WIRE*) missions; for completeness, we also include our independent re-analysis of the *MOST* data.

## 2 OBSERVATIONS

An overview of the time sampling is provided by Table 1 and Fig. 1, while the data quality is illustrated in Fig. 2. Although of somewhat lower cadence and accuracy than the other datasets, the *SMEI* observations are noteworthy in that they span six years, with approximately eight months' almost continuous coverage annually, allowing us to examine the long-term behaviour of periodic signals, presumed to arise from pulsations.

### 2.1 *SMEI*

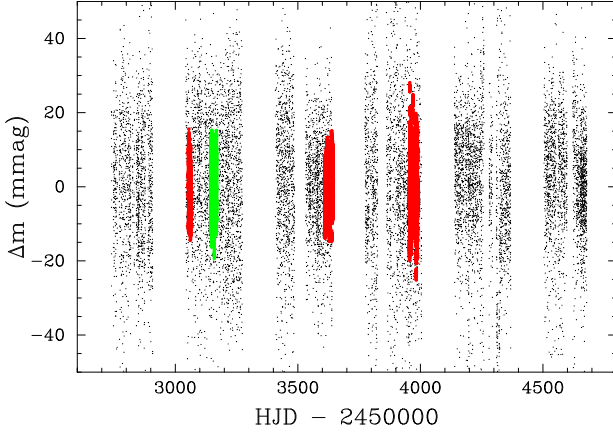
*SMEI* was one of two instruments on the *Coriolis* satellite, launched on 2003 January 6; data acquisition ceased on 2011 Sept 28. Designed to detect and forecast coronal mass ejections moving towards the Earth, *SMEI* had three imaging cameras, but camera 3 suffered a relatively high-temperature

\* i.howarth@ucl.ac.uk

<sup>1</sup> HD 149757

**Table 1.** Summary of observations.

Satellite	Observation Period	<i>N</i>	Satellite	Observation Period	<i>N</i>
<i>SMEI</i>	2003 Feb 10 – Sept 25	1467	<i>WIRE</i>	2004 Feb 18 – Feb 27	6663
<i>SMEI</i>	2004 Feb 7 – Sept 25	2473	<i>WIRE</i>	2005 Aug 28 – Sept 30	40739
<i>SMEI</i>	2005 Feb 6 – Sept 25	2255	<i>WIRE</i>	2006 Aug 8 – Sept 9	28113
<i>SMEI</i>	2006 Feb 6 – Sept 26	2194			
<i>SMEI</i>	2007 Feb 7 – Sept 25	2340	<i>MOST</i>	2004 May 18 – June 11	9084
<i>SMEI</i>	2008 Feb 7 – Aug 1	2101			

**Figure 1.** Time distribution of  $\zeta$  Oph data. The extensive dataset is the *SMEI* results; the four shorter sequences, showing smaller dispersions in magnitude, are results from *WIRE* (red) and *MOST* (green, second cluster of points).

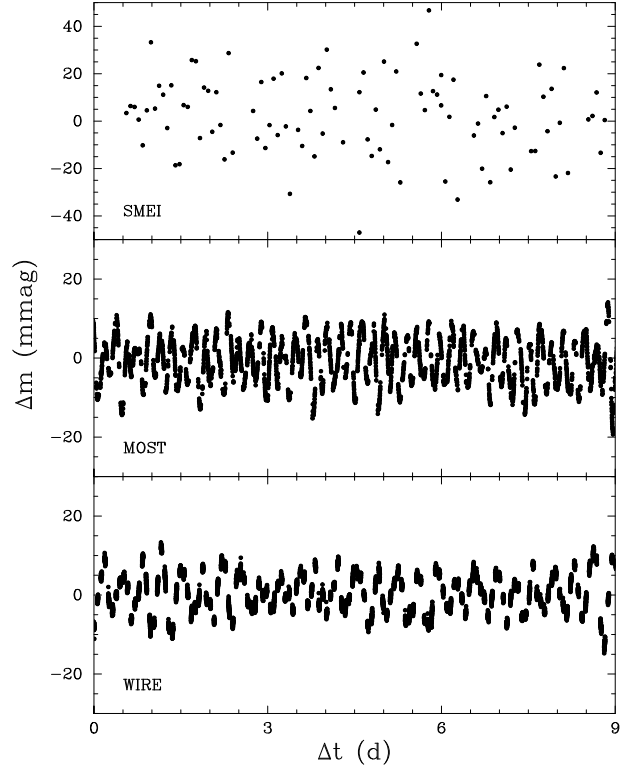
state, and as a result the quality of its photometric data is relatively poor. Here we only use results from cameras 1 and 2.

*SMEI* was capable of measuring millimagnitude variability down to  $\sim 6^{\text{mmag}}$ . The optical system was unfiltered, so the passband was dominated by the spectral response of the CCDs: the quantum efficiency peaked at 45% at 700 nm, falling to 10% at  $\sim 460$  and 990 nm. The cameras each had a field of view of  $60^\circ \times 3^\circ$ , and were mounted such that they scanned nearly the entire sky every 101 minutes. The duty cycle for the  $\zeta$  Oph time series is 46.6%, a typical value for *SMEI* photometry. Our  $\zeta$  Oph analysis uses data from six seasons, spanning  $\sim 5\frac{1}{2}$  years (Table 1), after which there is a falloff in data quality.

The *SMEI* instrument is fully described by Eyles et al. (2003), and a brief description of the data reduction can be found in Spreckley & Stevens (2008); other *SMEI*-based photometric investigations include studies of  $\alpha$  Boo,  $\beta$  UMi,  $\gamma$  Dor,  $\alpha$  Eri, Cepheid variables, and the magnetic CP star CU Vir (Tarrant et al. 2007, 2008a,b; Goss et al. 2011; Berdnikov & Stevens 2010; Pyper et al. 2013).

## 2.2 WIRE

The *WIRE* satellite was launched in 1999. Its main infrared camera never came into operation due to loss of coolant soon after launch, but the star tracker was successfully employed from 1999 to 2006 to measure precise light-curves of bright stars, in a passband roughly corresponding to  $V + R$ , determined by the CCD response (Bruntt & Buzasi 2006;

**Figure 2.** Illustrative data sequences, starting HJD 2 453 150 (*SMEI*, *MOST*) and 2 453 620 (*WIRE*).

Bruntt & Southworth 2008). *WIRE* observed  $\zeta$  Oph in three runs, and we extracted photometry using the *WIRE* pipeline (Bruntt et al. 2005).

## 2.3 MOST

The *MOST* satellite is a photometric instrument dedicated to asteroseismic observations (Walker et al. 2003), and again had a broad spectral response ( $\sim 350$ – $700$ nm). *MOST* observed  $\zeta$  Oph for 23 days in 2004; these observations have already been discussed in detail by Walker et al. (2005).

## 3 TIME-SERIES ANALYSIS

All *SMEI* photometry shows long-term variations of instrumental origin (e.g., Goss et al. 2011). These were removed with a ten-day running-mean filter, and a time-series analysis performed on the corrected data using PERIOD04 (Lenz

& Breger 2005). Fig. 3 shows the date-corrected discrete-fourier-transform amplitude spectrum (Ferraz-Mello 1981); although the formal Nyquist frequency imposed by the orbital period is  $7.086 \text{ d}^{-1}$ , the window function is very clean, and useful information can be extracted at somewhat shorter periods (into the frequency domain explored by spectroscopic investigations). However, it is clear from Fig. 3 (and from other *SMEI*-based analyses) that the Sun-synchronous orbit of the satellite generates signals at frequencies of  $1 \text{ d}^{-1}$  and multiples thereof. Any astrophysical signals which occur at these frequencies cannot be reliably identified in the *SMEI* data alone.

### 3.1 Summary of frequencies

‘Significant’ astrophysical signals (those with  $S/N \geq 4$  in the full *SMEI* dataset) are summarised in Table 2, where the tabulated errors on the frequencies and amplitudes have been calculated from Monte-Carlo simulations. The  $7.19 \text{ d}^{-1}$  signal identified spectroscopically by Reid et al. (1993) and Kambe et al. (1997), from observations obtained in 1989 and 1993, respectively, is present in the photometry (and has therefore persisted, or recurred, over at least two decades), but none of the longer-period signals they report is recovered, with upper limits of  $\sim 0.1\text{--}0.2 \text{ mmag}$ . Walker et al. (2005) report additional signals at  $4.49$ ,  $5.18$ , and  $6.72 \text{ d}^{-1}$  in their spectroscopy (and *MOST* photometry); signals at these frequencies are also present in the *SMEI* results, although the last two are detected at only  $2\text{--}3\sigma$  significance.

The *WIRE* and *MOST* time series have been analysed in the same way, with results included in Table 2. The frequencies found in all three datasets are generally in good agreement, though not all frequencies are detectable at all epochs. In a few cases there are formally statistically significant differences in frequencies from different datasets, but it is not clear that these are astrophysically significant. For example, the  $5.18 \text{ d}^{-1}$  frequency in the 2006 *WIRE* dataset appears to be marginally lower than found in the full *SMEI* and *MOST* results, but the 2006 *SMEI* data alone, although of poorer quality than the *WIRE* results, support a higher value. Our interpretation of the data is, therefore, that there is no compelling evidence for variations in frequency for a given signal. To support this view, we show the power spectra season by season in Fig. 4. Essentially identical frequencies recur each year, but with large variations in amplitude.

### 3.2 Amplitude variability

We take advantage of the long, uniform time series obtained by *SMEI* to examine these changes in amplitude in greater detail. Fig. 5 shows the semi-amplitudes (and periods) determined from 50-d data segments, at 25-d steps, for the strongest signals in the *SMEI* photometry. As already evident from Fig. 4, variability in signal amplitude on timescales of order hundreds of days is the norm; most clearly, the signal at  $5.18 \text{ d}^{-1}$  has a large amplitude during 2003 and 2004, but becomes practically undetectable over the course of the 2005 observing season, remaining at a very low level for the remainder of the period under consideration. (These conclusions are not artefacts of the data; the noise level and fill factor of the *SMEI* data show no impor-

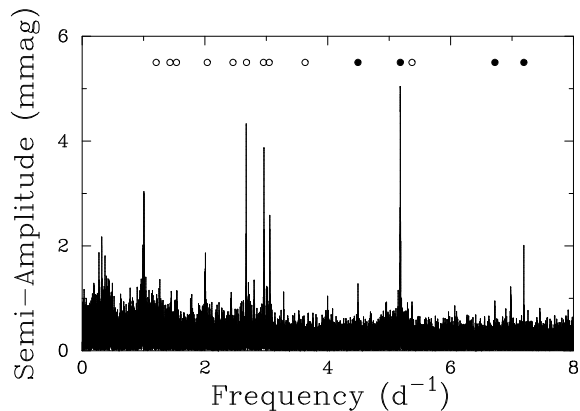


**Figure 3.** Amplitude spectrum of  $\zeta$  Oph from *SMEI* photometry. The open circles indicate frequencies reported by Walker et al. (2005) from *MOST* photometry; filled circles also have spectroscopic identifications (Reid et al. 1993; Kambe et al. 1997; Walker et al. 2005). Signals at integer multiples of  $1 \text{ d}^{-1}$  are assumed not to be astrophysical in origin.

tant changes over this time interval, and the *WIRE* results exhibit the same trends, though in less detail.)

In principle, it would be of obvious interest to investigate the phase stability of the signals; in practice, the phasing errors across the extensive timespan studied here are too large to allow firm conclusions in this regard, other than to state that there is no evidence for significant phase drift.

## 4 DISCUSSION

### 4.1 Signal duration

The strongest signal found here, at  $5.18 \text{ d}^{-1}$  ( $4^{\text{h}}53^{\text{m}}$ ), was first reported by Balona (1992), whose ground-based Strömgren photometry indicated a semi-amplitude of  $\sim 0^{\text{m}}01$  in 1985. He was unable to recover this period in subsequent, relatively sparse, observations from the 1987–90 seasons, concluding both that there was no periodicity that lasted more than one season, and that the short-period variations were not stable.

The extensive, high-quality satellite photometry now available allows us to revise these conclusions; signal amplitudes are indeed strongly variable, on timescales  $\sim O(10^2 \text{ d})$ , but, while undetectable at some epochs, the same periods may be recoverable in datasets separated by three decades. Balona (1992) also found a  $2.66 \text{ d}^{-1}$  signal (among other tentative identifications) in 1989 observations; this very probably matches the  $2.67 \text{ d}^{-1}$  signal observed in the *SMEI*, *WIRE* and *MOST* datasets, again emphasizing that at least some signals may be present over decades (cf.  $7.19 \text{ d}^{-1}$ ; §3.1), though whether they persist continuously, sometimes below detection thresholds, remains moot.

### 4.2 Emission-line episode

Spectroscopy that is contemporaneous with our photometry is available in the BeSS archive (Neiner et al. 2011; dispersions of  $\sim 0.1\text{--}0.3 \text{ \AA/pixel}$ ) and from Ondřejov Observatory (Harmanec, personal communication;  $\sim 0.25 \text{ \AA/pixel}$ );

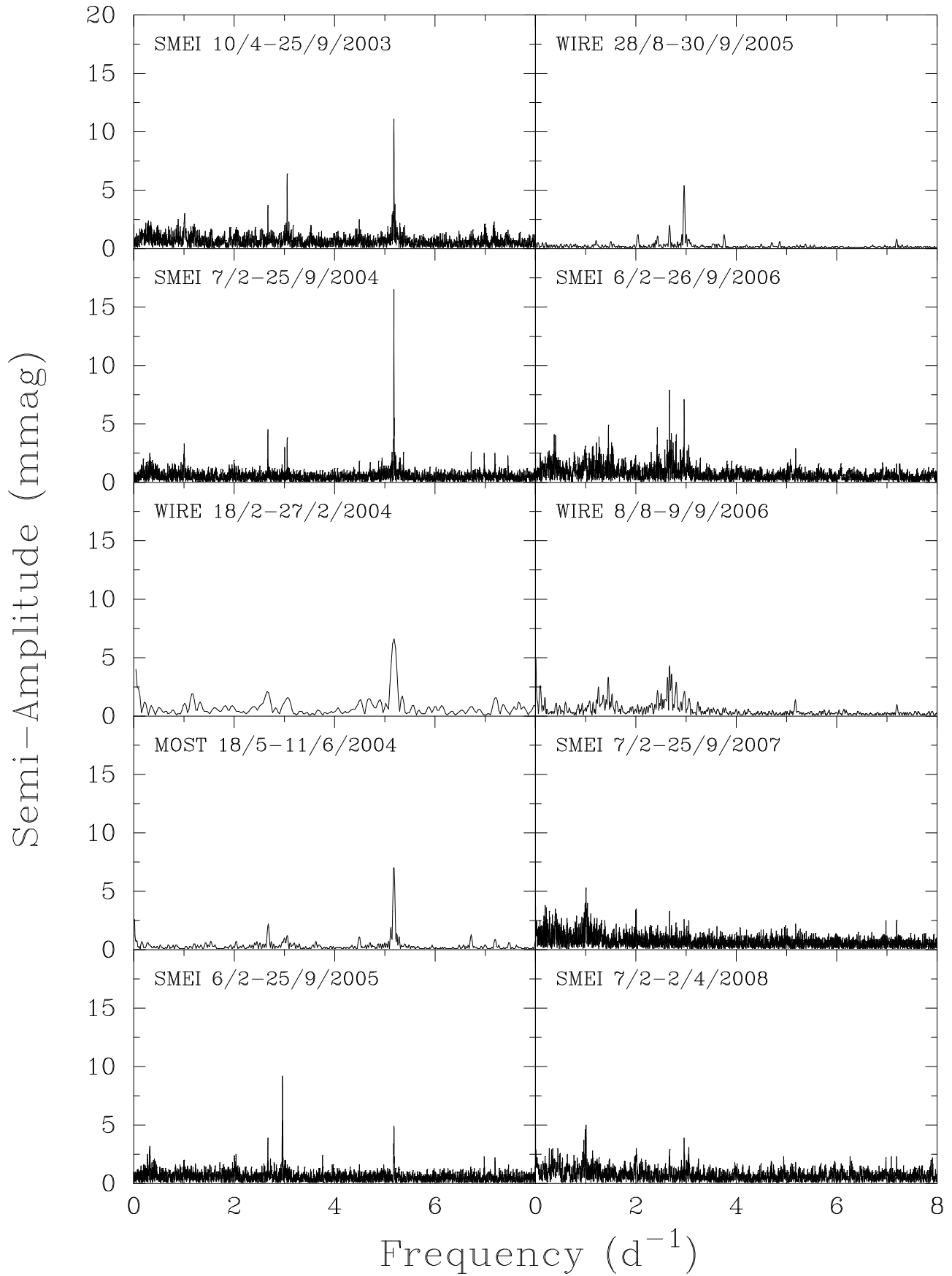


**Figure 4.** Power spectra by observing season, ordered chronologically by date of first observation.

**Table 2.** Signals identified with  $\gtrsim 4\sigma$  confidence at frequencies 1–8 d<sup>−1</sup>. (The Nyquist frequency for the *SMEI* photometry is 7.1 d<sup>−1</sup>.)

<i>SMEI</i> 2003–8		<i>WIRE</i> 2004		<i>MOST</i> 2004		<i>WIRE</i> 2005		<i>WIRE</i> 2006	
Frequency (d <sup>−1</sup> )	Amplitude (mmag)	Frequency (d <sup>−1</sup> )	Amplitude (mmag)	Frequency (d <sup>−1</sup> )	Amplitude (mmag)	Frequency (d <sup>−1</sup> )	Amplitude (mmag)	Frequency (d <sup>−1</sup> )	Amplitude (mmag)
		1.165(2)	1.77(5)	–	–	–	–	–	–
		–	–	–	–	–	–	1.2537(2)	2.82(3)
		–	–	–	–	–	–	1.3549(3)	2.02(3)
		–	–	–	–	–	–	1.4480(2)	3.40(3)
		–	–	–	–	2.0385(2)	1.13(1)	–	–
		–	–	–	–	–	–	2.3816(4)	1.54(3)
		–	–	–	–	2.4334(3)	0.90(1)	2.4297(2)	2.55(3)
		–	–	–	–	–	–	2.6269(2)	2.43(3)
2.67137(2)	4.3(3)	2.648(1)	2.16(5)	2.6762(4)	2.24(4)	2.6706(1)	1.86(1)	2.6800(1)	4.63(3)
		–	–	–	–	–	–	2.7014(1)	4.31(3)
		–	–	–	–	–	–	2.8060(2)	3.51(3)
2.96041(2)	4.0(3)	–	–	2.953(1)	0.76(4)	2.96120(5)	5.32(1)	2.9581(3)	2.31(3)
		–	–	3.0153(8)	1.11(4)	–	–	–	–
3.05498(3)	5.1(3)	3.085(2)	1.49(5)	3.0481(6)	1.50(4)	3.0557(3)	0.90(1)	3.0578(4)	1.51(3)
		–	–	–	–	3.7588(2)	1.16(1)	–	–
4.49194(5)	1.3(2)	–	–	4.4906 (8)	1.07(4)	–	–	–	–
		–	–	–	–	4.7092(5)	0.53(1)	–	–
		–	–	–	–	4.8650(5)	0.53(1)	–	–
5.18082(1)	5.1(3)	5.1796(5)	6.68(5)	5.1805(1)	7.22(4)	–	–	5.1760(8)	1.32(3)
[5.371(2)	0.9(4)]	–	–	5.371(1)	0.70(4)	–	–	–	–
[6.719(8)	1.0(3)]	–	–	6.7209(7)	1.28(4)	–	–	–	–
7.19196(5)	2.0(3)	7.205(4)	1.6(1)	7.196(3)	0.85(9)	7.1917(7)	0.83(3)	7.20(2)	0.9(1)

the formal signal-to-noise ratios are typically a few hundred per sample. We have corrected these spectra for absorption in the Earth’s atmosphere by division by a scaled high-resolution reference telluric spectrum before measuring equivalent widths.

The data show that  $\zeta$  Oph underwent an emission episode in summer 2006, similar to that illustrated by Ebbets (1981, his Fig. 1). Our H $\alpha$  equivalent-width measurements are included in Fig. 5. There is a suggestion that the emission-line episode may have been accompanied (or slightly preceded) by simultaneous small increases in the amplitudes of the 2.67, 2.96, and 5.18 d<sup>−1</sup> signals. Unfortunately, with only one emission-line episode during the course of our observations, it is not possible to draw firm conclusions from this coincidence; nevertheless, it is suggestive that the two lower frequencies attained the greatest amplitudes recorded in our photometry at that time.

The largest amplitudes, and largest changes in amplitude, are recorded for the higher-frequency 5.18 d<sup>−1</sup> photometric signal, and there is no clear association between that signal and any emission-line activity. However, Walker et al. (2005) showed that this frequency could very plausibly correspond to a first-overtone *radial* mode (exciting non-radial modes that give rise to the spectroscopic line-profile variability). The potential pulsation mechanism for producing decretion disks discussed by Cranmer (2009; see also Ando 1986) relies on the injection of angular momentum into the upper atmosphere by *non-radial* modes. Although there are as yet no mode identifications for the 2.67 and 2.96 d<sup>−1</sup> signals (which do not have published spectroscopic counterparts), it therefore remains plausible that the emission-line episode could be causally associated with increases in amplitudes of non-radial modes.

## 5 CONCLUSION

Data from the *SMEI*, *WIRE*, and *MOST* satellites have been analysed to investigate periodic signals in broad-band optical photometry of the Oe star  $\zeta$  Oph obtained over a span of almost 6 years. We confirm multiperiodic variability at the  $\sim 10$  mmag level and, for the first time, track systematic changes in signal amplitudes on timescales of order  $\sim 10^2$  d; some signals, while not continuously detectable, are nevertheless present in observations separated by 20–30 years. There is tentative evidence of a photometric signature of the 2006 emission-line episode; although no direct correspondence is evident between overall photometric and spectroscopic activity, this *may* reflect different roles of radial and non-radial modes in the formation of a decretion disk.

## ACKNOWLEDGEMENTS

KJFG, IRS, WJC, and YE acknowledge the support of STFC. IDH is a Jolligoode Fellow. This work has made use of the BeSS database, operated at the Observatoire de Meudon; we thank the contributing observers C. Buil, J. Guarroflo, C. Neiner, E. Pollmann, and O. Thizy, together with Petr Harmanec, who kindly provided spectra from Ondřejov, and Steve Spreckley, who assisted with the *SMEI* data reduction. Our anonymous referee’s remarks were constructively stimulating.

## REFERENCES

- Ando H., 1986, A&A, 163, 97
- Balona L. A., 1992, MNRAS, 254, 404

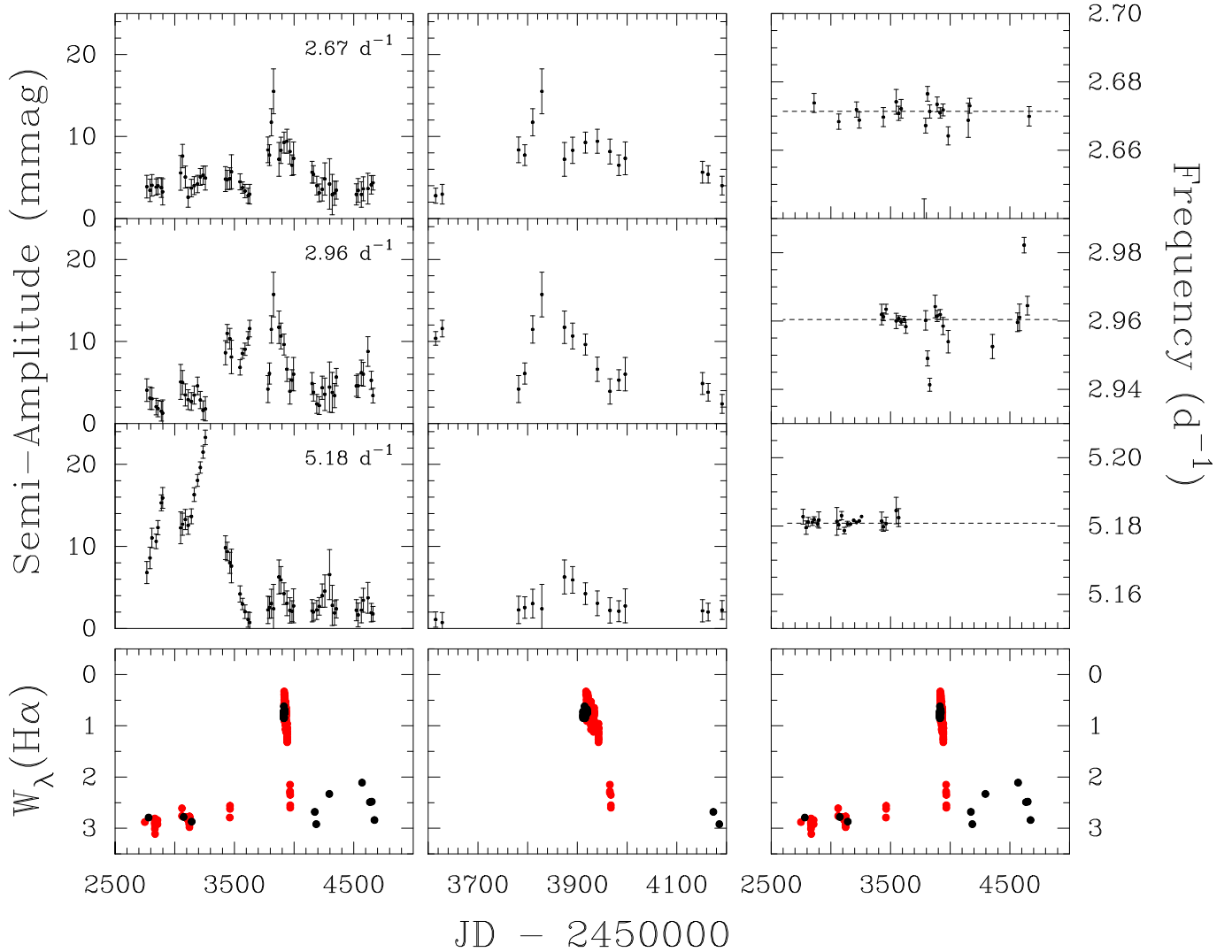


**Figure 5.** (Left, top three panels) amplitudes for the strongest signals in the *SMEI* dataset, evaluated for 50-d data segments at 25-d intervals; (centre) zoom of data during the 2006 emission-line episode. (Right) frequencies for dates when the amplitude was  $\geq 4\times$  its error, where the errors have been estimated analytically, following Montgomery & O'Donoghue (1999; these are lower limits to true uncertainties). Dashed horizontal lines indicate the mean frequencies determined from the full *SMEI* dataset. The bottom panels show our H $\alpha$  equivalent-width measurements (red: Ondřejov spectra; black: BeSS database); the cluster of points around JD...3930 with  $W_\lambda \lesssim 2\text{\AA}$  corresponds to an emission-line episode.

Berdnikov L. N., Stevens I. R., 2010, in C. Sterken, N. Samus, & L. Szabados ed., *Variable Stars, the Galactic halo and Galaxy Formation Search for Random Fluctuations in Periods of Short-period Cepheids*. p. 207  
 Bruntt H., Buzasi D. L., 2006, *MemSAI*, 77, 278  
 Bruntt H., Kjeldsen H., Buzasi D. L., Bedding T. R., 2005, *ApJ*, 633, 440  
 Bruntt H., Southworth J., 2008, *Journal of Physics Conference Series*, 118, 01201  
 Cranmer S. R., 2009, *ApJ*, 701, 396  
 Ebbets D., 1981, *PASP*, 93, 119  
 Eyles C. J., Simnett G. M., Cooke M. P., Jackson B. V., Buffington A., Hick P. P., Waltham N. R., King J. M., Anderson P. A., Holladay P. E., 2003, *Solar Physics*, 217, 319  
 Ferraz-Mello S., 1981, *AJ*, 86, 619  
 Goss K. J. F., Karoff C., Chaplin W. J., Elsworth Y.,

Stevens I. R., 2011, *MNRAS*, 411, 162  
 Howarth I. D., Smith K. C., 2001, *MNRAS*, 327, 353  
 Kambe E., Ando H., Hirata R., 1993, *A&A*, 273, 435  
 Kambe E., Hirata R., Ando H., Cuypers J., Katoh M., Kennelly E. J., Walker G. A. H., Stefl S., Tarasov A. E., 1997, *ApJ*, 481, 406  
 Lenz P., Breger M., 2005, *Communications in Asteroseismology*, 146, 53  
 Montgomery M. H., O'Donoghue D., 1999, *Delta Scuti Star Newsletter*, 13, 28  
 Neiner C., de Batz B., Cochard F., Floquet M., Mekkas A., Desnoux V., 2011, *AJ*, 142, 149  
 Pyper D. M., Stevens I. R., Adelman S. J., 2013, *MNRAS*, 431, 2106  
 Reid A. H. N., Bolton C. T., Crowe R. A., Fieldus M. S., Fullerton A. W., Gies D. R., Howarth I. D., McDavid D., Prinja R. K., Smith K. C., 1993, *ApJ*, 417, 320

- Sota A., Maíz Apellániz J., Walborn N. R., Alfaro E. J., Barbá R. H., Morrell N. I., Gamen R. C., Arias J. I., 2011, *ApJS*, 193, 24
- Spreckley S. A., Stevens I. R., 2008, *MNRAS*, 388, 1239
- Tarrant N. J., Chaplin W. J., Elsworth Y., Spreckley S. A., Stevens I. R., 2007, *MNRAS*, 382, L48
- Tarrant N. J., Chaplin W. J., Elsworth Y., Spreckley S. A., Stevens I. R., 2008a, *A&A*, 483, L43
- Tarrant N. J., Chaplin W. J., Elsworth Y. P., Spreckley S. A., Stevens I. R., 2008b, *A&A*, 492, 167
- van Leeuwen F., 2007, *A&A*, 474, 653
- Villamariz M. R., Herrero A., 2005, *A&A*, 442, 263
- Vogt S. S., Penrod G. D., 1983, *ApJ*, 275, 661
- Walker G., Matthews J., Kuschnig R., Johnson R., Rucinski S., Pazder J., Burley G., et al., 2003, *PASP*, 115, 1023
- Walker G. A. H., Kuschnig R., Matthews J. M., Reegen P., Kallinger T., Kambe E., et al., 2005, *ApJL*, 623, L145
- Walker G. A. H., Yang S., Fahlman G. G., 1979, *ApJ*, 233, 199